Insight in bipolar mania: evaluation of its heterogeneity and correlation with clinical symptoms

Rafael de Assis da Silva, Daniel C. Mograbi, Jaqueline Bifano, Cristina M.T. Santana, Elie Cheniaux

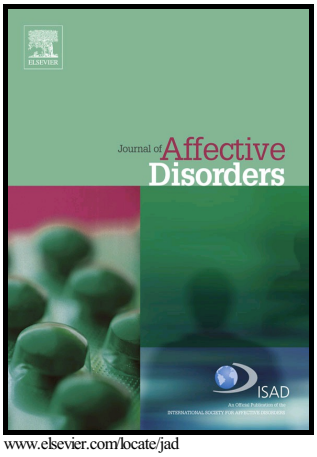

www.elsevier.com/locate/jad

PII: S0165-0327(16)30178-1
DOI: http://dx.doi.org/10.1016/j.jad.2016.04.019
Reference: JAD8166

To appear in: *Journal of Affective Disorders*

Received date: 4 February 2016
Revised date: 16 March 2016
Accepted date: 11 April 2016

Cite this article as: Rafael de Assis da Silva, Daniel C. Mograbi, Jaqueline Bifano, Cristina M.T. Santana and Elie Cheniaux, Insight in bipolar mania evaluation of its heterogeneity and correlation with clinical symptoms, *Journal of Affective Disorders,* http://dx.doi.org/10.1016/j.jad.2016.04.019

Temperature and concentration effects on upconversion photoluminescence properties of Ho^{3+} and Yb^{3+} codoped $0.67Pb(Mg_{1/3}Nb_{2/3})O_3$-$0.33PbTiO_3$ multifunctional ceramics

Zhen Liu[a], Guicheng Jiang[a,*], Ruixue Wang[a], Chengkai Chai[a], Limei Zheng[a], Zhiguo Zhang[a], Bin Yang[a,*] and Wenwu Cao[a,b]

[a] Condensed Matter Science and Technology Institute, Harbin Institute of Technology, Harbin 150080, China

[b] Department of Mathematics and Materials Research Institute, The Pennsylvania State University, Pennsylvania 16802, USA

*Corresponding author. Tel./fax: +86 451 86402771, email address: gjiang@hit.edu.cn (G. Jiang), binyang@hit.edu.cn (B. Yang)

Abstract

Ho^{3+} and Yb^{3+} codoped lead magnesium niobate-lead titanate (PMN-PT) ceramics with various doping concentration have been fabricated by conventional solid reaction method. Under the excitation of 980 nm laser, as-synthesized samples exhibit bright yellow-green upconversion (UC) luminescence. Their UC photoluminescence properties were investigated by the emission spectra with respect to various concentration of Ho^{3+} and Yb^{3+}. Results show that optimal luminescent concentration was obtained in $0.67Pb(Mg_{1/3}Nb_{2/3})O_3$-$0.33PbTiO_3$ ceramics codoped with 0.5 mol% Ho^{3+} and 2 mol% Yb^{3+} (abbreviated as 67PMN-33PT:2Yb,0.5Ho). The possible mechanism of UC emission was discussed by energy level diagrams of Ho^{3+} and Yb^{3+} ions according to the dependence of integrated intensity of UC emission bands on pumping power. Furthermore, the temperature dependence of UC emission intensity of 67PMN-33PT:2Yb,0.5Ho sample was investigated in detail in

the range of 25-180 ºC under excitation by a 980 diode laser. According to Arrhenius formula, the fitting result of the effect of temperature on integrated intensity of emission band was coinciding well with the experiment results. It is shown that the emission intensity depends strongly on temperature, which has excellent relative sensitivity with its maximum value of 0.77% K^{-1} at 93 ºC. These indicate that the 67PMN-33PT:2Yb,0.5Ho ceramic may be useful for temperature sensing and optical-electrical devices as a multifunctional material.

Key words: Rare-earth; upconversion photoluminescence; multifunctional ceramics; temperature sensing.

1. Introduction

In recent years, upconversion (UC) luminescent materials have attracted much attention due to their wide application in color displays [1,2], compact solid lasers devices [3], optical sensors [4-7], high efficiency solar cells [8,9] and bioimaging [10,11]. UC luminescence is a typical process in which low energy photons are absorbed by UC luminescent materials and then high energy photons are generated. UC materials are usually composed of rare-earth (RE) ions and host matrix materials. The transition electrons of RE ions in the host matrix of UC materials are often in 4f orbitals, which are shielded by the outer electrons in 5d6s orbitals. Although the transition between different 4f energy levels is parity forbidden by selecting rules, the crystal field around the dopant ions was affected by crystal structure of the host, which made the transition possible, then generated long-lived and line like emission spectrum. In order to get strong upconversion light, it is important to choose optimum

rare-earth ions as luminescence center and sensitizer. Among the RE ions, Ho^{3+} ion is the most interesting one, which has abundant energy levels in the spectroscopic range of ultraviolet to near infrared (NIR) spectrum. Yb^{3+} ion was often used as sensitizer of Ho^{3+} ion, which has large absorption cross section of NIR. Moreover, Ho^{3+} and Yb^{3+} codoped materials excited by 980 nm laser often exhibited green and red emissions [12].

Ferroelectric ceramic is a kind of important functional material with excellent piezoelectric, ferroelectric and pyroelectric properties. $0.67Pb(Mg_{1/3}Nb_{2/3})O_3$-$0.33PbTiO_3$ (abbreviated as 67PMN-33PT) ceramic is a typical ferroelectric material that exhibits excellent piezoelectricity and high dielectric constant with the morphotropic phase boundary (MPB) composition [13,14]. It was widely used in various high-tech area such as ultrasonic transducers, actuators and sensors [15-17]. As a kind of host material, PMN-PT has the advantages of excellent chemical, physical, and thermal stabilities compared to current glasses and fluorides. To maintain the ferroelectric properties while getting the new function of ferroelectric ceramics, RE ions doped ferroelectric ceramics have been investigated as multifunctional materials that can achieve electro-mechano-optical conversions [18].

In this work, the Yb^{3+} and Ho^{3+} codoped PMN-PT ceramics were first fabricated. To suppress the formulation of second phase and get the strong luminescence, Yb^{3+} concentration was fixed at 2 mol%. The structure and UC photoluminescence properties of Ho^{3+} and Yb^{3+} codoped PMN-PT ceramics as a function of Ho^{3+} concentration were investigated, and the optimum combination with the strong UC

emission was obtained. Furthermore, temperature and pumping power dependent UC luminescent properties of 2 mol% Yb^{3+} and 0.5 mol% Ho^{3+} codoped PMN-PT (abbreviated as 67PMN-33PT:2Yb,0.5Ho) ceramic were also discussed in detail. The integrated emission intensity at 550 nm decrease remarkably about 70% as the temperature increasing from 25 ˚C to 180 ˚C, and the experiment data was analyzed by Arrhenius formula fitting, which describes the trend line of experiment result.

2. Experimental procedure

Yb^{3+} and Ho^{3+} codoped 67PMN-33PT ceramics were prepared by conventional solid reaction method [19]. Here, the nominal concentration of Yb^{3+} ions was fixed at 2 mol% and Ho^{3+} ions was x mol% (x = 0.05, 0.1, 0.2, 0.5, 1 and 2). These samples were abbreviated as 67PMN-33PT:2Yb,xHo.

High pure powders of PbO, MgO, Nb_2O_5, TiO_2, Yb_2O_3 and Ho_2O_3 were used as raw materials. The stoichiometric MgO and Nb_2O_5 were mixed and milled with alcohol in agate mortar for 2 hours, then the slurry were heated at 120 ˚C in heating oven to get the dry mixed powder. After that, precursor powder of $MgNb_2O_6$ was calcined at 1000 ˚C for 4 hours using the mixed powder of MgO and Nb_2O_5. Subsequently, the acquired precursor was mixed with PbO, TiO_2, Yb_2O_3 and Ho_2O_3 according to the designed ratio with an addition of 2 wt% excess PbO to compensate the lead loss during calcinating and sintering, and then regrinded in agate mortar for 2 hours. Mixed powder was calcined at 950 ˚C to obtain the perovskite phase. After calcining, the powders were mixed with 5% poly vinyl alcohol solution (PVA), and

then uniaxially pressed into disks with 13 mm in diameter. All the pellets were burned out the PVA binder at 550 ˚C for 1 hour and then sintered at 1200 ˚C for 4 hours in a sealed alumina crucible to get the ferroelectric ceramics.

The phase structure of all ceramics were characterized by X-Ray diffraction (XRD, D/max 2400, Rigaku Corporation, OR) with CuKa radiation (λ = 0.15418 nm) in the 2θ range from 10˚ to 60˚. The upconversion luminescence spectra were examined by Zolix-SBP300 grating spectrometer equipped with a CR131 photomultiplier tube. The emission spectra were measured in the range of 500 nm to 800 nm with the scanning step of 1 nm. A commercial 980 nm diode laser was used as pump light source. For temperature-dependent photoluminescence measurements, the temperature of 67PMN-33PT:2Yb0.5Ho was controlled by a heating microscope stage (THMS600 Linkam) from room temperature to 180 ˚C. Before emission data collection, the temperature was held for 3 minutes to avoid violent disturbance of the temperature.

3. Result and discussion

XRD patterns of 67PMN-33PT doping with and without 2 mol% Yb^{3+}, x mol% Ho^{3+} ceramics were shown in Fig. 1 in the 2θ range of 10˚ to 60˚. As shown in the diffraction patterns, pure perovskite phase without secondary phase can be obtained when $x \leq 0.5$. The secondary phase (marked by arrows) emerged as the concentration of Ho^{3+} above 0.5 mol%. Those indicated that the crystal structure of 67PMN-33PT was influenced by increasing the substitution of Ho^{3+} and Yb^{3+} in perovskite lattice. The perovskite diffraction peaks were also indexed by profile (JCPDS Card

No.81-8061) and labelled in the figure. The {200} peaks do not show significant splitting, but with shoulders on the right sides, indicating that the composition of our samples are located at the MPB region [13].

Room temperature UC emission spectra of PMN-PT ceramics with variant Ho^{3+} concentration and fixed Yb^{3+} concentration excited by a 980 nm diode laser were presented in Fig. 2a. The inset of Fig. 2a shows strong yellow-green UC photoluminescence observed by naked eyes in daylight. There are three emission bands near 541 nm, 654 nm and 756 nm respectively in the UC emission spectra. Among the three emission bands, the green light centered at 550 nm originated from $(^5F_4, ^5S_2) \rightarrow {}^5I_8$ transition is the most strong, the red luminescence located at 650 nm associated with $^5F_5 \rightarrow {}^5I_8$ transition is weaker, and the near infrared emission from $(^5F_4, ^5S_2)$ to $^5I_7$ transition near 756 nm is the lowest. The integrated intensity of each emission band as a function of Ho^{3+} doping concentration is displayed in Fig. 2b. It can be observed that the intensity of all three bands increased with Ho^{3+} concentration below 0.5 mol%. The highest photoluminescence intensity at 0.5 mol% Ho^{3+} is twice higher than the lowest concentration doping. Further increase of Ho^{3+} concentration leads to decrease of the UC emission integrated intensity. This is because the Ho^{3+} ion is the activator in the luminescence process, as the concentration of Ho^{3+} increases, the concentration of luminescent center raises up. However, there is a doping limit that emissions stop increasing. This phenomena is the so-called concentration quenching. As known, the distances between rare-earth ions changed while they were doped into host materials. As the doping concentration of Ho^{3+} ions exceeded 0.5

mol%, the distances between Ho^{3+}-Ho^{3+}, Ho^{3+}-Yb^{3+} and Yb^{3+}-Yb^{3+} in the PMN-PT ceramics became shorter. As a result, the interaction between rare-earth ions got stronger, the cross relaxation occurred and the energy transfer efficiency decreased so that the luminescence became weaker.

In order to get further insight into the mechanism of UC emission process of Ho^{3+}, Yb^{3+} codoped 67PMN-33PT ceramics, the UC emission spectra of the 67PMN-33PT:2Yb,0.5Ho ceramic as a function of pump power were examined. The dependence of UC photoluminescence of PMN-PT:2Yb,0.5Ho ceramic on pump power of the 980 nm laser diode were shown in Fig. 3. It can be seen that the peak value of each emission band increases gradually with incident power. When the pump power was 80 mW, the luminescent intensity value was one order lower than that at 472 mW. The relationship between the UC emission intensity and pump power can be described by the following formula [20,21].

$$I \propto P^m \quad (1)$$

Where I is the integrated intensity of UC luminescence spectrum, P is pump power of incident light from diode laser. As the math expression (Eq. (1)), integrated intensity of emission band is proportional to the exponent of pump power. The index m is the number of required absorbing photons for exciting the electron from the ground state to the excited state. Inset of Fig. 3 shows the logarithm coordinates of experiment data point and the fitting curve of ln I versus ln P, and m can be determined from the slope of each curve. Results show that the m value of green, red and near infrared emissions are 2.10, 2.03 and 2.06, separately. Therefore, the UC emissions of these three

processes of Yb^{3+} and Ho^{3+} doped 67PMN-33PT ceramics excited by 980 nm laser are all involved in two-photon processes. The energy level diagram of RE is shown in Fig. 4. As shown in the diagram, the possible population processes in Yb^{3+} and Ho^{3+} codoped PMN-PT ceramics can be described as follows: Under the 980 nm laser excitation, Yb^{3+} ions were excited from ground state $^2F_{7/2}$ to excited state $^2F_{5/2}$ by the ground state absorption. Subsequently, the population of the state $^5I_7$ of Ho^{3+} ions could be achieved by the energy transfer (ET) from Yb^{3+} to Ho^{3+}. Then the Ho^{3+} ions absorb more photons to populate the $^5F_5$ and the coupling state of ($^5F_4$, $^5S_2$) through excitation state absorption (ESA). There are two routes to generate the red emission: one is that the intermediary level $^5I_6$ of Ho^{3+} is populated by ground state absorption (GSA) from $^5I_8$, and then relaxes to $^5I_7$ by non-radiative transition. Subsequently, the excited level $^5F_5$ is populated by absorbing another photon via ESA. At last, the electrons leap from $^5F_5$ to the $^5I_8$ state with red emission. The other possible route is that the level of $^5I_6$ is populated from $^5I_8$ as route one. Then the ($^5F_4$, $^5S_2$) level is populated by absorbing another photon. The population of $^5F_5$ level is achieved by non-radiation process, and then the transition from $^5F_5$ to $^5I_8$ generates the red emission. For green UC luminescence, the emission is attributed to the transition from ($^5F_4$, $^5S_2$) to $^5I_8$ state. In addition, few electrons leaped from ($^5F_4$, $^5S_2$) into $^5I_7$ state, emitting the infrared luminescence.

Furthermore, to investigate the influence of temperature on photoluminescence properties, the UC luminescence spectra of PMN-PT:2Yb,0.5Ho ceramic were measured in the spectra range of 500 nm to 800 nm as a function of temperature in the

range from 25 ˚C to 180 ˚C. As shown in Fig. 5, the emission intensities of green, red and near infrared light are all sensitive to temperature in this system. It can be observed that the luminescent intensity decreased gradually with temperature due to the increased non-radiative relaxation of electrons between rare earth energy levels. In addition, the inset of Fig. 5 shows temperature dependence of luminescence intensity ratio ($I_{654\ nm}/I_{550\ nm}$). The ratio increased gradually with temperature. This is due to the fact that possibilities of non-radiative transition of ($^5F_4$, $^5S_2$) → $^5F_5$ become stronger as the temperature increases by the assisting of the phonon of the matrix. It also can be evaluated by the non-radiative decay rate (W), which is mathematically written as:

$$W(T) = W(0)[\frac{e^{h\nu/kT}}{e^{h\nu/kT}-1}]^{\Delta E/kT} \quad (2)$$

Where T is absolute temperature; W(T) and W(0) are the non-radaitive decay rate at temperature T and 0 K, respectively; ΔE represents the energy gap of two levels; $h\nu$ is the phonon energy of host matrix and k is the Boltzmann constant [22].

To further investigate the process of thermal quenching of Yb^{3+}, Ho^{3+} codoped 67PMN-33PT ceramics, we analyzed the dependence of temperature and normalized integrated intensity of three emission bands separately. As known, the temperature dependent emission properties can be described by a modified Arrhenius equation [23, 24]:

$$I(T) = \frac{I_0}{1 + Ae^{-\frac{\Delta E}{kT}}} \quad (3)$$

Where A is a fitting constant, ΔE is active energy of thermal quenching, k is the Boltzmann constant, I_0 is the initial intensity at 0 K, and I(T) is the intensity at

temperature T. We use the Matlab software to fit the experimental data. The integrated intensity of each band was normalized by the integrated value at 25 ˚C in our experiment. The experimental results and fitting curve were shown in Fig. 6. It can be observed the experimental data can be well fitted by the modified Arrhenius equation. During the fitting process, the activation energies are 0.1518 eV for green emission, 0.1115 eV for red emission and 0.1478 eV for infrared emission, respectively. Furthermore, the relative sensitivity S is a very important parameter to evaluate the performance of the sensor, which can be described by the following formula:

$$S = \left| \frac{1}{I} \frac{dI}{dT} \right| \quad (4)$$

This equation means that the relative change of emission intensity with respect to temperature variation. The calculated result was described in Fig. 7. As shown, the relative sensitivity reached the maximum value of 0.0077 K^{-1} at 366 K (about 93 ˚C). This temperature sensitivity can be comparable that of Yb^{3+}-Er^{3+} doped $CaWO_4$ (0.0073 K^{-1}), Yb^{3+}-Er^{3+} doped Gd_2O_3 nanophosphor (0.0039 K^{-1}) and Er^{3+} doped $Sr_2Bi_4Ti_5O_{18}$ (0.0042 K^{-1}) [25-27]. Hence, the Yb^{3+} and Ho^{3+} codoped 67PMN-33PT multifunctional ceramics possess good temperature sensitivity, and can be used as a potential temperature sensor material based on UC photoluminescence.

4. Conclusion

In summary, Yb^{3+} and Ho^{3+} codoped 67PMN-33PT multifunctional ceramics were synthesized by conventional solid-state reaction method. The pure

perovskite-phase samples were obtained when the concentration of Ho^{3+} was lower than 0.5 mol%. Under the excitation of 980 nm laser, all doped samples exhibited strong yellow-green emissions. By comparing the upconversion emission spectra with respect to the different doping condition, the optimal luminescent concentration of Ho^{3+} was found at 0.5 mol% when Yb^{3+} was fixed at 2 mol%. Based on pump power dependent emission intensities, the green, red, and near-infrared emissions are all two-photon processes. As the temperature increasing from 25 ˚C to 180 ˚C, the upconversion emission intensity decreases dramatically about 70%, which gives a maximal temperature sensitivity value of 0.0077 K^{-1} at 366 K (about 93 ˚C). These results illuminate that the Yb^{3+} and Ho^{3+} codoped 67PMN-33PT multifunctional ceramic could be an excellent candidate for applying in temperature sensing.

Acknowledgments

This work was financially supported by the National Key Basic Research Program of China (No. 2013CB632900), the National Natural Science Foundation of China (Nos. 11404321, 51572056, 51572055, and 81571720), and the Fundamental Research Funds for the Central Universities and Program for Innovation Research of Science in Harbin Institute of Technology (No. Q201509).

References

[1] E. Downing, L. Hesselink, J. Ralston, R. Macfarlane, A three-color, solid-state, three-dimensional display, Science 273 (1996) 1185.

[2] X.Y. Li, Y.L. Yu and Z.Q. Zheng, A temperature dependent investigation of upconversion emission in Er^{3+}: PLZT transparent ceramic, Ceram. Int. 42 (2016) 490−494.

[3] H, Chen, B. Yang, Y. Sun, M. Zhang, Y. Sui, Z.G. Zhang, W.W. Cao, Investigation on upconversion photoluminescence of Bi_3TiNbO_9:Er^{3+}:Yb^{3+} thin films, J. Lumin. 131 (2011) 2574−2578.

[4] S.S Zhou, G.C. Jiang, X.Y. Li, X.T. Wei, Y.H. Chen, C.K. Duan, M. Yin, Strategy for thermometry via Tm^{3+}-doped $NaYF_4$ core-shell nanoparticles, Opt. Lett. 39 (2014) 6687−6690.

[5] F. Vetrone, R. Naccache, A. Zamarro, A.J. de la Fuente, F.S. Rodriguez, L.M. Maestro, E.M. Rodriguez, D. Jaque, J.G. Sole, J.A. Capobianco, Temperature sensing using fluorescent nanothermometers, ACS. Nano. 4 (2010) 3254−3258.

[6] G.C. Jiang, S.S. Zhou, X.T. Wei, Y.H. Chen, C.K. Duan, M. Yin, B. Yang and W.W. Cao, 794 nm excited core-shell upconversion nanoparticles for optical temperature sensing, RSC. Adv. 6 (2016) 11795–11801.

[7] H. Suo, C.F. Guo, Z. Yang, S.S. Zhou, C.K. Duan, M. Yin, Thermometric and optical heating bi-functional properties of upconversion phosphor $Ba_5Gd_8Zn_4O_{21}$:Yb^{3+}/Tm^{3+}, J. Mater. Chem. C 3 (2015) 7379–7385.

[8] H. Lian, Z. Hou, M. Shang, D. Geng, Y. Zhang, and J. Lin, Rare earth ions doped phosphors for improving efficiencies of solar cells, Energy. 57 (2013) 270−283.

[9] H.Q. Wang, M. Batentschuk, A. Osvet, L. Pinna and C.J. Brabec, Rare, Earth Ion Doped upconversion materials for photovoltaic applications, Adv. Mater. 23 (2011) 2675−2680.

[10] G.C. Jiang, J. Pichaandi, N.J.J. Johnson, R.D. Burke and F.C.J.M. van Veggel, An effective polymer cross-linking strategy to obtain stable dispersions of upconverting $NaYF_4$ Nanoparticles in Buffers and Biological Growth Media for Biolabeling Applications, Langmuir 28 (2012) 3239−3247.

[11] J. Zhou, Z. Liu and F. Li, Upconversion nanophosphors for small-animal imaging, Chem. Soc. Rev. 41. (2012) 1323−1349.

[12] G. Ding, F. Gao, G. Wu, D. Bao, Bright up-conversion green photoluminescence in Ho^{3+}-Yb^{3+} co-doped $Bi_4Ti_3O_{12}$ ferroelectric thin films, J. Appl. Phys. 109 (2011) 123101.

[13] A.K. Singh, D. Pandey, Evidence for MB and MC phases in the morphotropic phase boundary region of (1−x)[$Pb(Mg_{1/3}Nb_{2/3})O_3$]−x$PbTiO_3$:A Rietveld study. Phys. Rev. B 67 (2002) 480−485.

[14] B. Noheda, D.E. Cox, G. Shirane, J. Gao, Z.G. Ye, Phase diagram of the ferroelectric relaxor (1−x) $PbMg_{1/3}Nb_{2/3}O_3$−x$PbTiO_3$, Phys. Rev. B 65 (2002) 144101.

[15] F. Kochary, M.D. Aggarwal, A.K. Batra, R. Hawrami, D. Lianos, A. Burger, Growth and electrical characterization of the lead magnesium niobate-lead titanate (PMN-PT) single crystals for piezoelectric devices. J. Mater. Sci. Mater. El. 19 (2008) 1058−1063.

[16] S. Zhang, F. Li, High performance ferroelectric relaxor-$PbTiO_3$ single crystals: Status and perspective, J. Appl. Phys. 111 (2012) 031301.

[17] E.W. Sun, W.W. Cao, Relaxor-based ferroelectric single crystals: Growth, domain engineering, characterization and applications, Prog. Mater. Sci. 65 (2014) 124–210.

[18] X. Wang, C.N. Xu, H. Yamada, K. Nishikubo, X.G. Zheng, Electro-Mechano-Optical Conversions in Pr^{3+}-Doped $BaTiO_3$–$CaTiO_3$ Ceramics, Adv. Mater. 17 (2005) 1254−1258.

[19] P. Kumar, S Sharma, S. Singh, O.P. Thakur, C. Prakash, T.C. Goel, Structural and electrostrictive behaviour in PMN-PT (68:32) ceramics, Ferroelectrics 326 (2005) 55−60.

[20] T. Wei, X.D. Wang, C.Z. Zhao, T.B. Zhang, F.M Yang, W.B. Wang, Y.J. Ma, Enhanced upconversion photoluminescence and dielectric properties of Er- and Zr-codoped strontium bismuth niobate ceramics, Ceram. Int. 41 (2015) 12364−12370.

[21] P. Du, L.H. Luo, J.S. Yu, Low-temperature thermometry based on upconversion emission of Ho/Yb-codoped $Ba_{0.77}Ca_{0.23}TiO_3$ ceramics, J. Alloy. Compd. 632 (2015) 73−77.

[22] H. Suo, C.F. Guo, W.B. Wang, T. Li, C.K. Duan, M. Yin. Mechanism and stability of spectrally pure green up-conversion emission in Yb^{3+}/Ho^{3+} co-doped $Ba_5Gd_8Zn_4O_{21}$ phosphors, Dalton. T. 45 (2016) 2629−2636.

[23] V. Bachmann, A. Meijerink, C. Ronda, Luminescence properties of $SrSi_2AlO_2N_3$ doped with divalent rare-earth ions, J. Lumin. 129 (2009) 1341−1346.

[24] N. Feng, Y. Tian, L. Wang, Q. Shi, P. Huang, Band structure, energy transfer and temperature-dependent luminescence of novel blue emitting $KBaYSi_2O_7$: Eu^{2+} phosphor, J. Alloy. Comp. 654 (2016) 133−139.

[25] W. Xu, Z.G. Zhang, W.W. Cao, Excellent optical thermometry based on short-wavelength upconversion emissions in Er^{3+}/Yb^{3+} codoped $CaWO_4$, Opt. Lett. 37 (2012) 4865−4867.

[26] S.K. Singh, K. Kumar, S.B. Rai, Er^{3+}/Yb^{3+} codoped Gd_2O_3 nanophosphor for optical thermometry, Sens. Actuator A 149 (2009) 16–20.

[27] T. Wei, Z. Dong, C.Z. Zhao, Y.J. Ma, T.B. Zhang, Y.F. Xie, Z.P. Li, Up-conversion luminescence and temperature sensing properties in Er-doped ferroelectric $Sr_2Bi_4Ti_5O_{18}$, Ceram. Int. 42 (2016) 5537–5545.

Figure captions

Fig. 1. XRD patterns of PMN-PT ceramics doping with 2 mol% Yb^{3+} and x mol% Ho^{3+} (↓ represent the secondary phase of $Yb_2Ti_2O_5$).

Fig. 2(a) UC emission spectra of PMN-PT:2Yb,xHo ceramics excited by 980 nm laser with 281 mW. Inset is the photograph of PMN-PT:2Yb,0.5Ho ceramic excited by 980 nm laser taken by digital camera in daylight. (b) Integrated emission intensities of PMN-PT:2Yb, xHo ceramics as a function of Ho^{3+} concentration.

Fig. 3. UC emission spectra of PMN-PT:2Yb,0.5Ho ceramics as a function of pump power. Inset shows pump power dependence of the upconversion emission intensity of PMN-PT:2Yb,0.5Ho ceramic at 550 nm, 654 nm and 756 nm.

Fig. 4. Energy level diagrams of Ho^{3+} and Yb^{3+} in PMN-PT ceramic.

Fig. 5. UC emission spectra of PMN-PT:2Yb,0.5Ho ceramic at various temperature (Inset is temperature dependence of fluorescence intensity ratio of $I_{654\ nm}/I_{550\ nm}$).

Fig. 6. Dependence of normalized emission intensity at 550 nm of PMN-PT:2Yb,0.5Ho ceramic on temperature (Red line is the result fitted by Arrhenius formula).

Fig. 7. Relative sensitivity of PMN-PT:2Yb,0.5Ho ceramic at various temperature calculated by Eq. (3).

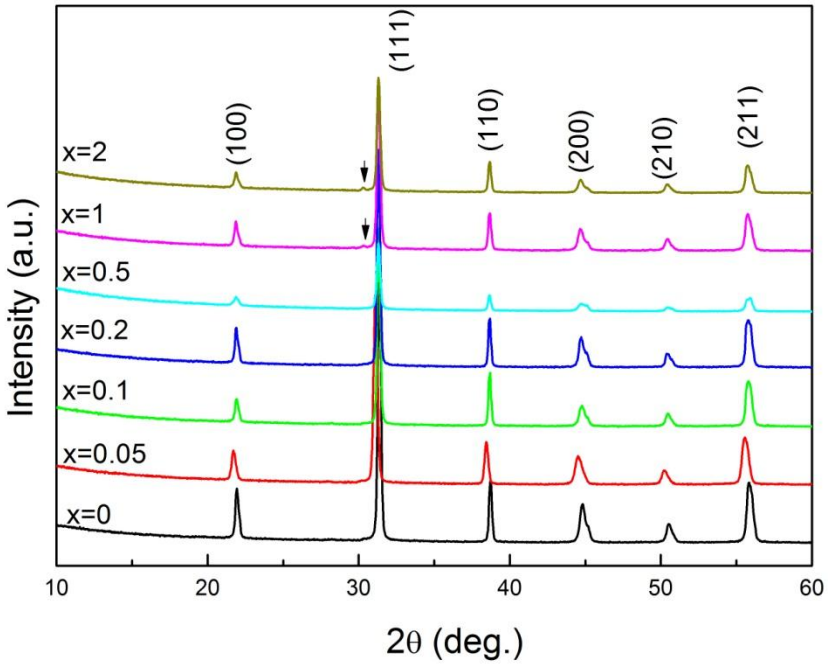

Fig. 1. XRD patterns of PMN-PT ceramics doping with 2 mol% Yb^{3+} and x mol% Ho^{3+} (↓ represent the secondary phase of $Yb_2Ti_2O_5$).

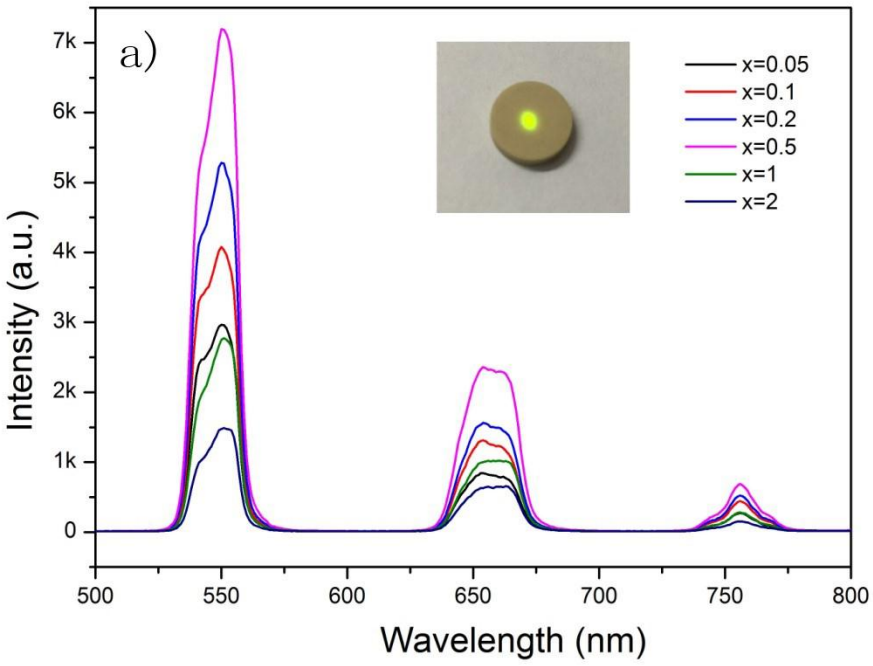
a)
x=0.05
x=0.1
x=0.2
x=0.5
x=1
x=2
Intensity (a.u.)
Wavelength (nm)
0
1k
2k
3k
4k
5k
6k
7k
500
550
600
650
700
750
800

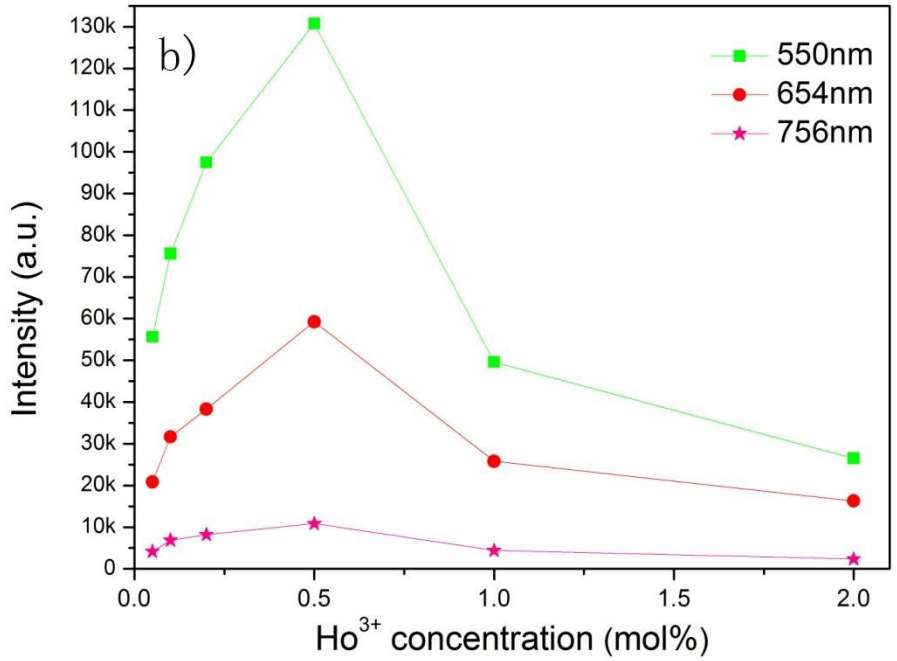

Fig. 2(a) UC emission spectra of PMN-PT:2Yb,xHo ceramics excited by 980 nm laser with 281 mW. Inset is the photograph of PMN-PT:2Yb,0.5Ho ceramic excited by 980 nm laser taken by digital camera in daylight. (b) Integrated emission intensities of PMN-PT:2Yb, xHo ceramics as a function of Ho^{3+} concentration.

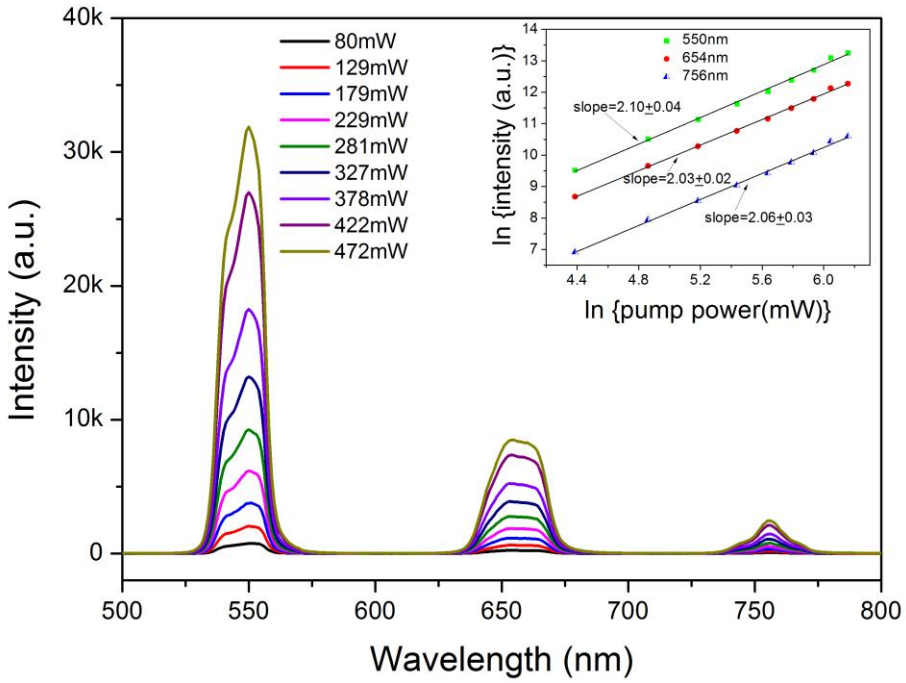

Fig. 3. UC emission spectra of PMN-PT:2Yb,0.5Ho ceramics as a function of pump power. Inset shows pump power dependence of the upconversion emission intensity of PMN-PT:2Yb,0.5Ho ceramic at 550 nm, 654 nm and 756 nm.

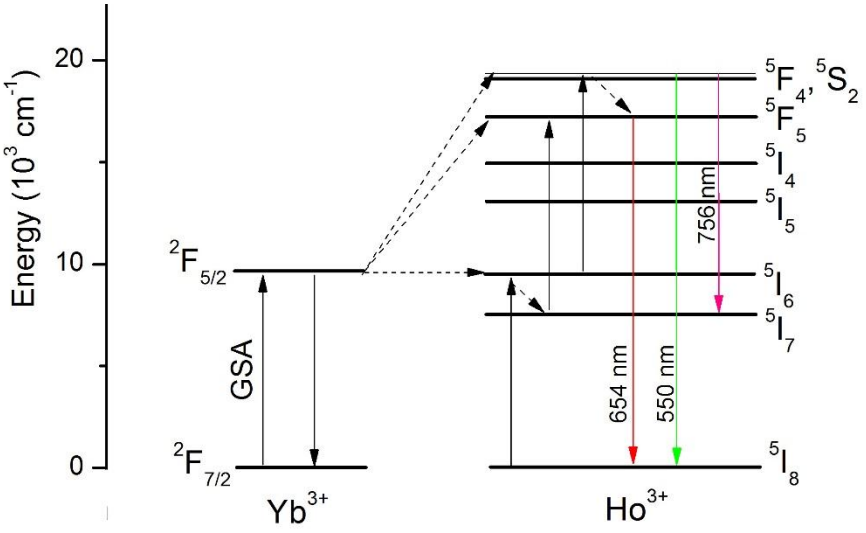

Fig. 4. Energy level diagrams of Ho^{3+} and Yb^{3+} in PMN-PT ceramic.

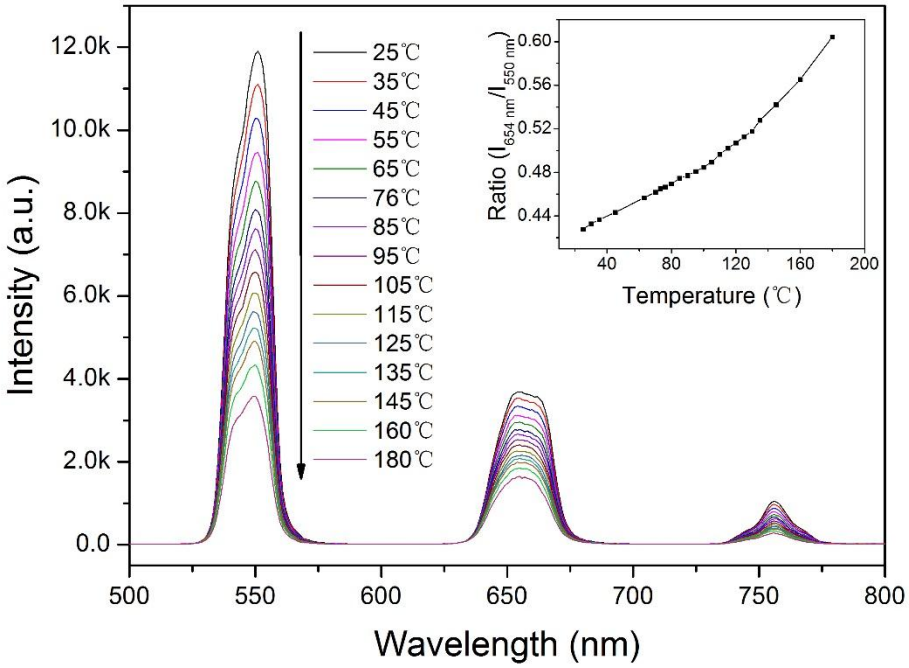

Fig. 5. UC emission spectra of PMN-PT:2Yb,0.5Ho ceramic at various temperature (Inset is temperature dependence of fluorescence intensity ratio of $I_{654\ nm}/I_{550\ nm}$).

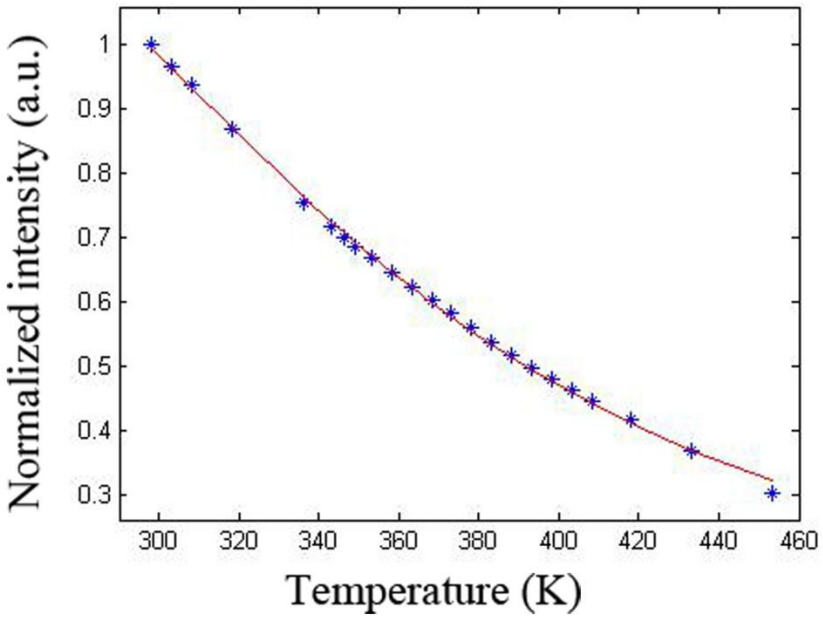

Fig. 6. Dependence of normalized emission intensity at 550 nm of PMN-PT:2Yb,0.5Ho ceramic on the temperature (Red line is the result fitted by Arrhenius formula).

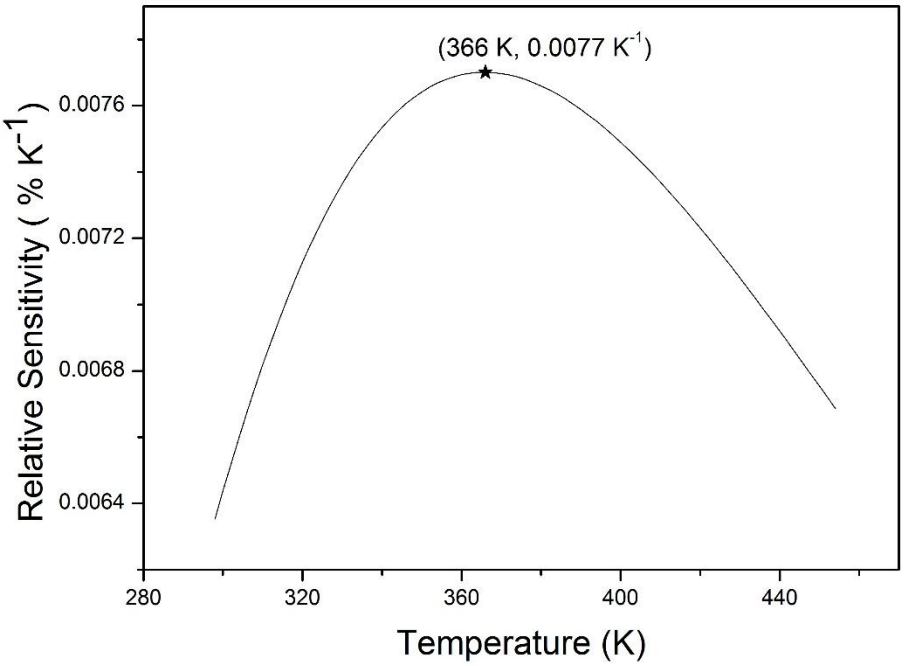

Fig. 7. Relative sensitivity of PMN-PT:2Yb,0.5Ho ceramic at various temperature calculated by Eq. (3).